Polymer Journal, Vol. 17, No. 7, pp 841—854 (1985)

Ex Vivo and *in Vitro* Blood Response to Surface-Modified Poly(styrene-*b*-butadiene-*b*-4-vinylpyridine) Triblock Polymers

Michael D. LELAH, Stuart L. COOPER, Hiroshi OHNUMA,* and Tadao KOTAKA*

Department of Chemical Engineering, University of Wisconsin-Madison, Madison, Wisconsin 53706, U.S.A.
**Department of Macromolecular Science, Osaka University, Toyonaka, Osaka 560, Japan*

(Received October 2, 1984)

ABSTRACT: An acute *ex vivo* canine series shunt technique, together with *in vitro* blood contact experiments, were used to study the blood compatibility of poly(styrene-*b*-butadiene-*b*-4-vinylpyridine) triblock polymers. The ABC type triblock polymers were solvent cast from different solvents, and were chemically modified by quaternization of the pyridine block, crosslinking of the butadiene block, and sulfonation of the styrene block. The surface properties of the polymers were studied using contact angle measurements, ESCA, ATR-IR, and SEM. The polymers cast from chloroform were more thromboresistant than those cast from a mixture of butyraldehyde and chloroform. The chloroform-cast materials were more hydrophilic and contained a greater proportion of surface nitrogen than those materials cast from the mixed solvent. Quaternization dramatically increased thrombogenicity. Subsequent crosslinking and sulfonation to produce a charge mosaic structure did not improve blood compatibility.

KEY WORDS ABC Type Triblock Copolymer / Charge Mosaic Polymer / Blood Compatibility / *Ex Vivo* Series Shunt / Surface Characterization /

The interaction of a polymer surface with blood usually results in the deposition of proteins, platelets and other blood components, which lead to the formation, growth and embolization of thrombi. The extent of this surface-induced thrombosis is determined in part by the nature of the polymer surface exposed to blood. Polymer surface properties that have been implicated in thrombosis include surface energy, charge, hydrophilicity, surface morphology, surface chemical composition and surface roughness.[1,2]

Multiphase block copolymers are interesting materials for blood-contacting applications. Phase separation results in domains with different chemical and physical properties which can lead to useful differential blood response characteristics. One multiphase copolymer family that has been extensively evaluated in blood contact studies is the family of the segmented polyurethane elastomers.[3-9] These $(AB)_n$-type polymers exhibit phase separation into hard (semicrystalline or glassy) and soft (elastomeric) domains. The ratio of the surface hard to soft segments appears to be an important parameter in determining blood response. A number of researchers have examined the blood compatibility of ABA triblock polymers.[10-13] Okano *et al.*[14] have proposed that the hydrophilic–hydrophobic balance between the blocks is the principal determinant of the thrombogenicity of these materials.

Only a few researchers have studied the blood compatibility of ABC-type triblock

polymers.[15,16] The poly(styrene-*b*-butadiene-*b*-4-vinylpyridine) ABC-type triblock polymers examined in this study are interesting in that selective modification of the individual blocks can be used to investigate the role of different surface properties in thrombogenesis. These triblock polymers can be cast from different solvents resulting in either ball-in-the-box or trilayer lamellar morphologies.[17-19] Selective quaternization of the poly(4-vinylpyridine) blocks, crosslinking of the polybutadiene blocks, and sulfonation of the polystyrene blocks result in the formation of a charge mosaic material[15,16,19-23] in which the polycations and polyanions are in separate domains or phases. It is necessary to use an ABC-type triblock polymer to prevent the formation of a polyion complex where pairs of cations and anions exchange from their respective microdomains. The middle polymer block (in this case the polybutadiene phase) is used to prevent ion exchange, and thus create a charge mosaic structure.

The different polymers examined were cast on the inner surface of polyethylene tubing. Selective chemical reactions were then carried out on these phase-separated materials. These surface modifications were extensively characterized using X-ray photoelectron spectroscopy (XPS or ESCA), contact angle measurements, attenuated total reflection infrared spectroscopy (ATR-IR) and scanning electron microscopy (SEM). This multiprobe approach was used to obtain as much information about the polymer surfaces as possible.

Ex vivo blood contact experiments were performed using an acute canine femoral arterio-venous series shunt that has been previously described[24,25] and used to study the interaction of different polymers with blood.[7,8,24,26] In this experiment, dynamic platelet and fibrinogen deposition profiles were determined using radiolabeling techniques. The series shunt arrangement allows for the investigation of a number of different materials using the same animal under similar physiological and hematological conditions. *In vitro* blood compatibility was assessed using a Lee–White clotting procedure[27] and an intrinsic coagulation pathway contact activation test specific to plasma kallikrein.[28]

EXPERIMENTAL

Polymers

The synthesis, morphology, and physical properties of the SBP triblock polymers composed of polystyrene (S), polybutadiene (B) and poly(4-vinylpyridine) (P) have been reported previously.[19,21] Table I lists molecular weight and volume compositions of the two polymers SBP-10 and SBP-12 used in this study. The weight fractions are related to the molecular weights by

$$X(\mathrm{S}) : X(\mathrm{B}) : X(\mathrm{P}) = M_n(\mathrm{S}) : M_n(\mathrm{B}) : M_n(\mathrm{P})$$

The volume fractions are related to molecular weight by

$$\phi(\mathrm{S}) : \phi(\mathrm{B}) : \phi(\mathrm{P}) = M_n(\mathrm{S})/\rho(\mathrm{S}) : M_n(\mathrm{B})/\rho(\mathrm{B}) : M_n(\mathrm{P})/\rho(\mathrm{P})$$

Table I. Molecular weight and volume compositions of the SBP samples studied

Sample	Number average mol wt ($\times 10^{-3}$)				Volume composition		
	M_n (S)	M_n (B)	M_n (P)	M_n (SBP)	ϕ (S)	ϕ (B)	ϕ (P)
SBP-10	30.1	14.3	28.5	72.9	0.41	0.23	0.36
SBP-12	13.3	15.6	24.2	53.0	0.24	0.34	0.42

with bulk densities $\rho(S)=1.05$, $\rho(B)=0.89$, and $\rho(P)=1.114\,g\,cm^{-3}$.

Coating Procedure

The polymers were solvent cast onto the inner lumen of 0.125″ (3.18 mm i.d.) polyethylene tubing (Intramedic® PE-350). The inner surface of the polyethylene tubing was first treated with chromic acid at room temperature for 2 h to increase its wettability. Following washing and drying, the polymer was cast from a 6% solution in either chloroform (designated as C) or in a 9:1 (v/v) mixture of butyraldehyde and chloroform (designated as B). Chloroform is a good solvent for the S and B blocks, but not for the P block, resulting in a ball-in-the-box bulk morphology.[19] The mixture is a good solvent for all the blocks and results in a trilayer lamellar bulk morphology.[19] The coating were dried at room temperature for 48 h under vacuum.

For the *in vitro* experiments, a conical polyethylene test tube (content, 10 ml; diameter, 16.5 mm; length, 105 mm) was used. The polymer of interest was cast from a 3% solution onto the inner surface of the polyethylene test tube.

Surface Modification

Quaternization of the pyridine block was accomplished using vapor-phase methyl bromide in the coated tube at 70°C for 48 h, followed by drying at room temperature for 48 h under vacuum. An excess of methyl bromide was used to insure complete reaction. The quaternized block is designated P(Q).

The poly(butadiene) (B) block on the coated tubing surface was crosslinked using a 5% (v/v) solution of freshly distilled sulfonyl chloride in methyl cyanide at room temperature for 150 min. The crosslinked surface was rinsed in hexane, acetone, and a 10% (v/v) solution of carbon disulfide in hexane, followed by drying for 48 h under vacuum. The crosslinked polybutadiene block is designated B(X).

The final step involved sulfonation of the polystyrene (S) block using HSO_3Cl vapor at room temperature for 30 min. Nitrogen gas was then used to displace the HSO_3Cl vapor and the sulfonated surface washed with 1,2-dichloroethane, acetone and water, and then dried in vacuum for 48 h at room temperature. The sulfonated polystyrene block is designated as S(S).

Surface Characterization

The surface properties of the polymers were determined directly on the coated surfaces.

ESCA

A Physical Electronic PHI 548 ESCA spectrometer with a 300 W Mg anode was used to obtain surface elemental compositions. A pass energy of 100 eV was used to obtain the data, which were corrected for atomic sensitivity.[29]

Contact Angle Measurements

The underwater captive bubble technique of Hamilton,[30] modified for the curved surfaces[31] was used here to obtain contact angle data. Air–water and octane–water (where possible) contact angles were determined on sections of the inner surfaces of the coated tubing. Where possible, the solid–water interfacial energy γ_{sw} was calculated using the harmonic mean approximation.[32]

ATR-IR

A Nicolet 7199 FT-IR coupled with a Barnes 300 ATR accessory were used to obtain the ATR-IR spectra. The coated tubings were sliced longitudinally and pressed against a 45° Germanium crystal. Spectra were collected at a resolution of $2\,cm^{-1}$.

SEM

Two scanning electron microscopes (SEM) were used: A JEOL 35C SEM at the University of Wisconsin operated at an accelerrating voltage of 10 kV, and a Hitachi S-430 SEM at the

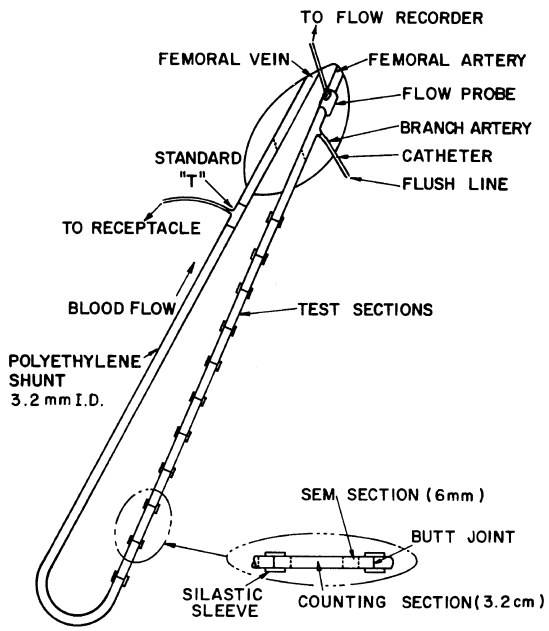

Figure 1. Details of the *ex vivo* cannulation site showing the joined series test section.

Osaka University operated at 20 kV were used to examine the topology of coated surfaces and to obtain a cross-sectional view of the coating.

Ex Vivo Blood Contact

The acute canine *ex vivo* femoral series shunt experiment used for the blood-compatibility studies has been described in detail previously.[24] Following hematological screening, dogs were injected with autologous ^{51}Cr-labeled platelets and ^{125}I-labeled purified fibrinogen. The femoral artery and vein in one leg were cannulated with the shunt which consisted of an entrance region, joined series test section and return section (Figure 1). The shunt was initially filled with a divalent cation-free Tyrodes solution to prevent blood-air contact. The joined series test section consisted of a series of randomized 5 cm section of each of the materials tested, and a polyethylene control joined using external silicon tubber connectors.

In the blood contact experiment, at the end of a predetermined blood contact time, the femoral artery was clamped shut. Blood was then flushed out of the shunt *via* a branch artery. The purpose of flushing was to remove the bulk blood in the shunt, leaving only blood components that had adhered to the tubing surface. Immediately following flushing, the joined series test section was removed, fixed with 2% glutaraldehyde, and then each material subdivided into section for gamma counting and SEM examination.

A new set of randomized test sections was inserted into the shunt for each blood contact time period, which ranged form 1/2 to 60 min. Three separate repeat surgeries using three different animals were performed. During each surgery, blood flow through the shunt was continuously monitored, and blood samples were taken at regular intervals for radioactivity determination, platelet count, fibrinogen level, hematocrit, and hematological function tests.[24] After correction for background and decay, platelet and fibrinogen deposition per unit area of surface was calculated from the radiolabeling and hematological data. SEM samples were obtained at each time point in order to characterize thrombus morphology on each surface.[25]

In Vitro Blood Contact

Canine blood coagulation time was measured using the method of Lee and White.[27] The contact phase activation of the intrinsic coagulation pathway was determined by measuring the rate of generation of kallikrein using a fluorometric technique developed by Matsuda *et al.*[28] *In vitro* examination of deposited platelets was performed using canine platelet rich plasma for 20 min contact. This was followed by fixation of the deposited platelets using 1% glutaraldehyde, and SEM examination.

RESULTS

Ex Vivo Blood Contact

Figures 2—5 show the temporal sequence of

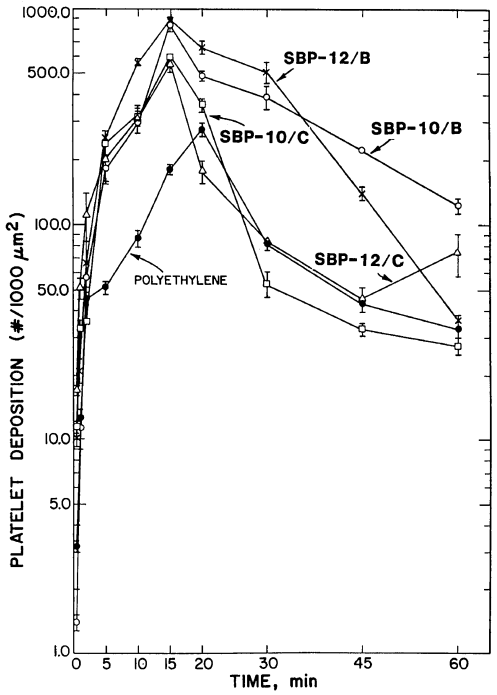

Figure 2. *Ex vivo* platelet deposition as a function of time for the unmodified polymers SBP-10/C, SBP-10/B, SBP-12/C, SBP-12/B and polyethylene.

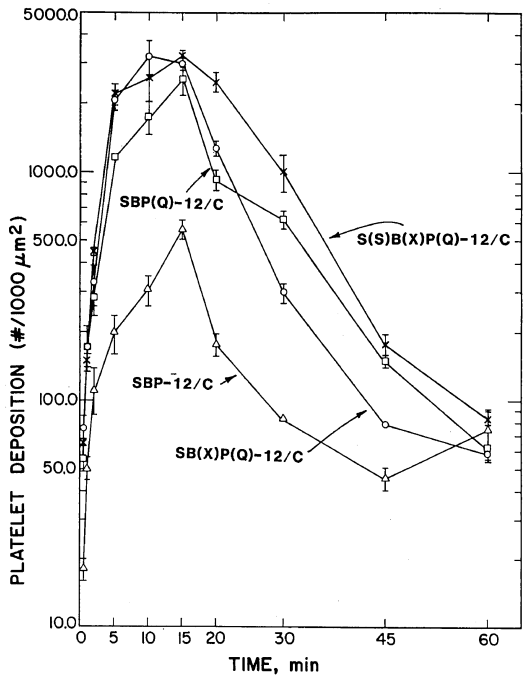

Figure 4. *Ex vivo* platelet deposition as a function of time for the chemically modified polymers SBP(Q)-12/C, SB(X)P(Q)-12/C and S(S)B(X)P(Q)-12/C, and for SBP-12/C.

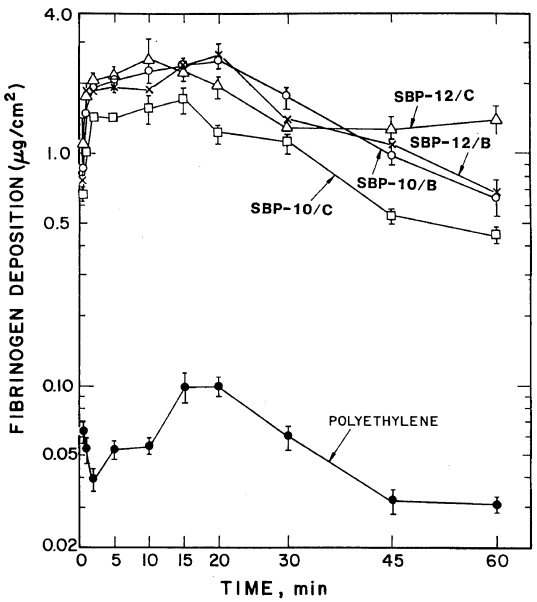

Figure 3. *Ex vivo* fibrinogen deposition as a function of time for the unmodified polymers SBP-10/C, SBP-10/B, SBP-12/C, SBP-12/B and polyethylene.

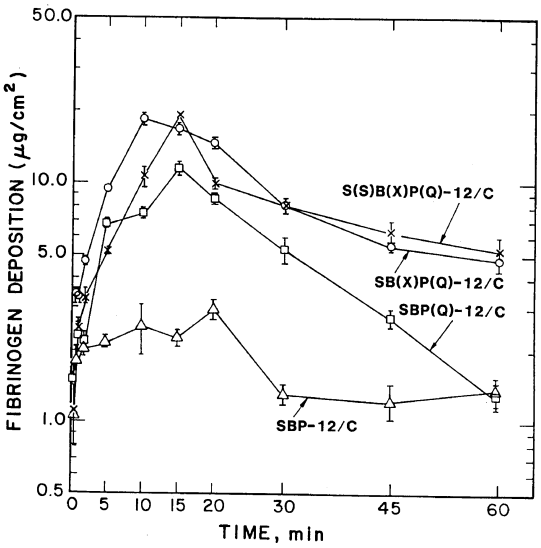

Figure 5. *Ex vivo* fibrinogen deposition as a function of time for the chemically modified polymers SBP(Q)-12/C, SB(X)P(Q)-12/C and S(S)B(X)P(Q)-12/C, and for SBP-12/C.

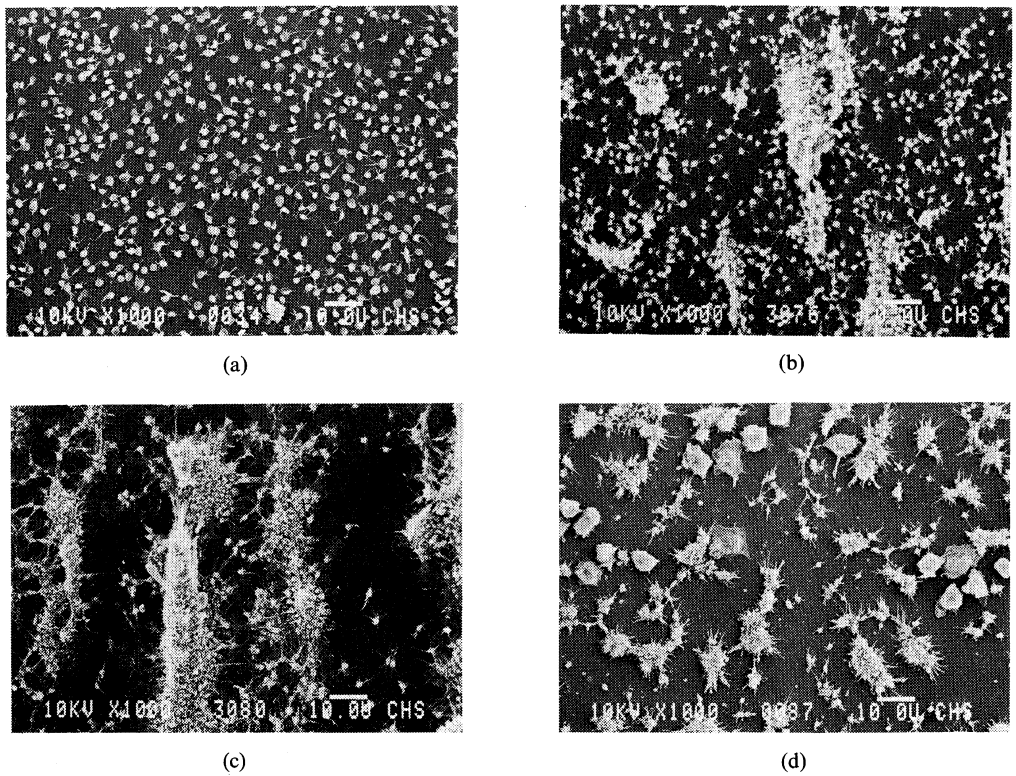

Figure 6. SEM micrographs of *ex vivo* blood contact on SBP-12/C at (a) 1 min, (6) 5 min, (c) 15 min, and (d) 60 min of blood contact, showing sequence of platelet deposition and aggregation, thrombus formation and embolization.

platelet and fibrinogen deposition per unit area over 60 min of blood contact for all surfaces studied. The error bars represent standard errors from the mean for the 3 experiments. The platelet and fibrinogen deposition results show a peak at 15—20 min of blood contact. This peak corresponds to the competition between thrombus deposition and embolization (embolus formation)[24] and thus can be used as one measure of the acute blood compatibility of the various materials. From Figures 2 and 3, the samples cast from chloroform (SBP-10/C and SBP-12/C) were more thromboresistant than those cast from a butyraldehyde/chloroform mixture (SBP-10/B and SBP-12/B). There appeared to be little difference in blood response between the SBP-10 and SBP-12 materials cast from the same solvent. From Figures 4 and 5, it can be seen that quaternization drastically increased thrombogenicity. Any effects of crosslinking and sulfonation were masked by the quaternization.

Figure 6 shows the morphology of the blood components on the surface of SBP-12/C at 1, 5, 15 and 60 min of blood contact. The micrographs, which typify the results on the unmodified polymers, (SBP-10/C, SBP-10/B, SBP-12/C, and SBP-12/B) show initial single platelet deposition with pseudopod extension, but little spreading at 1 min. By 5 min 10—20 μm size aggregates formed (Figure 6b), however again little platelet spreading is observed. At the peak time of 15 min large clumps about 50—100 μm in size can be observed (Figure 6c). At the end of the experiment, at 60 min of blood contact, most of the large

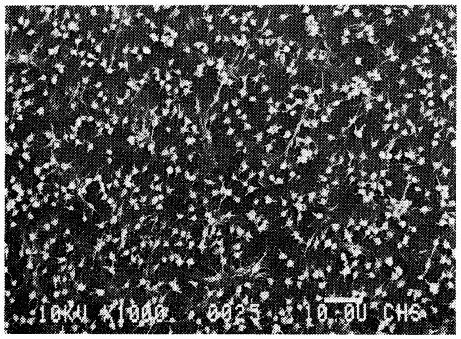

(a)

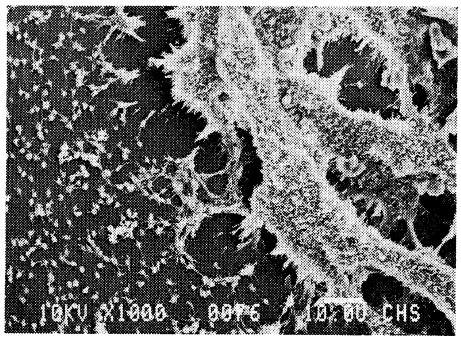

(b)

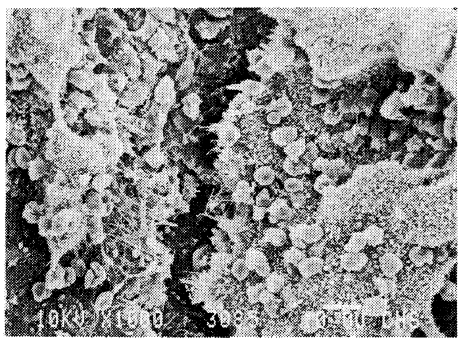

(c)

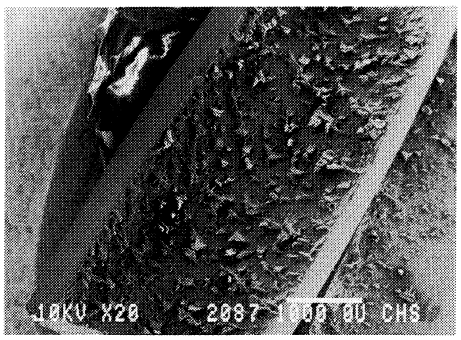

(d)

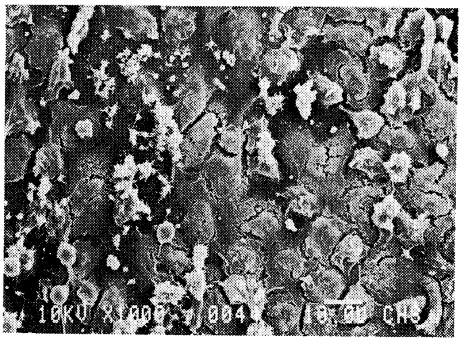

(e)

Figure 7. SEM micrographs of *ex vivo* blood contact on S(S)B(X)P(Q)-12/C at (a) 1 min, (b) 5 min, (c) and (d) 15 min, and (e) 60 min of blood contact. (c) shows a thrombus composed of platelets, red cells, leukocytes and fibrin. (d) shows a low magnification of the tubing with large thrombi covering the whole surface. (e) shows spread white cells covering the polymer surface with small platelet clumps.

thrombi have embolized, leaving small platelet aggregates (5—10 μm in size) and some white cells in various stages of activation (Figure 6d).

In contrast, the morphology of the blood components on S(S)B(X)P(Q)-12/C shown in Figure 7 indicates increased platelet deposition, consistant with the results in Figure 4. The sequence shown in Figure 7 is typical for the chemically modified materials. At 1 min of blood contact (Figure 7a), platelet spreading is extensive. The lower layer of platelets were often spread with the appearance of a well developed hyalomere. By 5 min large platelet thrombi are observed (Figure 7b). At the peak time of about 15 min, large thrombi (100—400 μm in size) covered the surface of the tubing. The thrombi are composed of platelets, white cells, red cells and an occasional fibrin network (Figure 7c). A view of a section of tubing at low magnification is shown in Figure 7d where the large thrombi can be seen to cover the whole surface. By 60 min of blood contact, most of the thrombi have embolized leaving smaller platelet clumps. The surface is however covered with spread leukocytes as shown in Figure 7e.

Table II. *In vitro* and *ex vivo* results normalized to polyethylene controls

Sample	*In vitro*		*Ex vivo*
	Lee–White clotting time ratio	Contact activation ratio	Peak platelet deposition ratio
SBP-10/C	—	—	2.1
SBP-10/B	—	—	3.0
SBP-12/C	0.68	0.76	2.0
SBP-12/B	0.72	0.86	3.1
SBP(Q)-12/C	0.36	1.36	9.0
SB(X)P(Q)-12/C	0.33	1.03	11.5
S(S)B(X)P(Q)-12/C	0.41	1.23	11.3
SBP(Q)-12/B	0.44	1.37	—
SB(X)P(Q)-12/B	0.46	1.07	—
S(S)B(X)P(Q)-12/B	0.53	0.98	—

In all the animal experiments, shunt blood flow rates were initially between 350 and 450 ml min^{-1} (wall shear rates of 1850—2400 s^{-1}). These rates decreased 20—30% around the peak deposition period (10—30 min) and then increased again to about 10% below original levels. Analysis of blood samples removed at 30 min intervals indicated little variation in platelet count, fibrinogen level, *in vivo* fibrinogen clottability, hematocrit, activated partial thromboplastin time, prothrombin time and euglobulin lysis time. Only the plasma protamine paracoagulation test turned positive toward the end of each surgery.

In Vitro Blood Contact

The *in vitro* blood contact results (normalized with a polyethylene control) and shown in Table II, together with peak platelet *ex vivo* results (also normalized with a polyethylene control). The Lee–White clotting time ratios show that the unmodified polymers have longer clotting times than the modified polymers, consistant with the *ex vivo* data. The contact activation ratios are also lower for the unmodified polymers, indicative of lower intrinsic coagulation activity on these materials. The *in vitro* results show the materials cast from butyraldehyde and chloroform to be more thromboresistant (longer Lee–White clotting time) than those cast from chloroform, but the *ex vivo* results show the opposite trend (greater platelet deposition).

Figure 8 shows *in vitro* platelet deposition on SBP-12/C, SBP(Q)-12/C, SB(X)P(Q)-12/C and S(S)B(X)P(Q)-12/C after 20 min of contact. The SEM results support the *in vitro* data in Table II. Single platelets with little activation can be seen on SBP-12/C (Figure 8a), while more extensively activated platelets and/or clumping are evident on the surfaces of the chemically modified polymers (Figures 8b—d).

Surface Characterization

Contact angle and ESCA data are shown in Table III. The solid–water interfacial energies (γ_{sw}) calculated for the unmodified polymers are low, indicating that they are rather hydrophilic surfaces. The chloroform cast materials (SBP-10/C and SBP-12/C) were slightly more hydrophilic than the same polymers cast from a mixture of butyraldehyde and chloroform. The ESCA N/C ratios for these materials indicate that the SBP-10/B and SBP-12/B coatings contain less surface nitrogen and thus less poly(4-vinylpyridine) phase on the surface than the same materials cast from chloroform. The poly(4-vinylpyridine) phase is

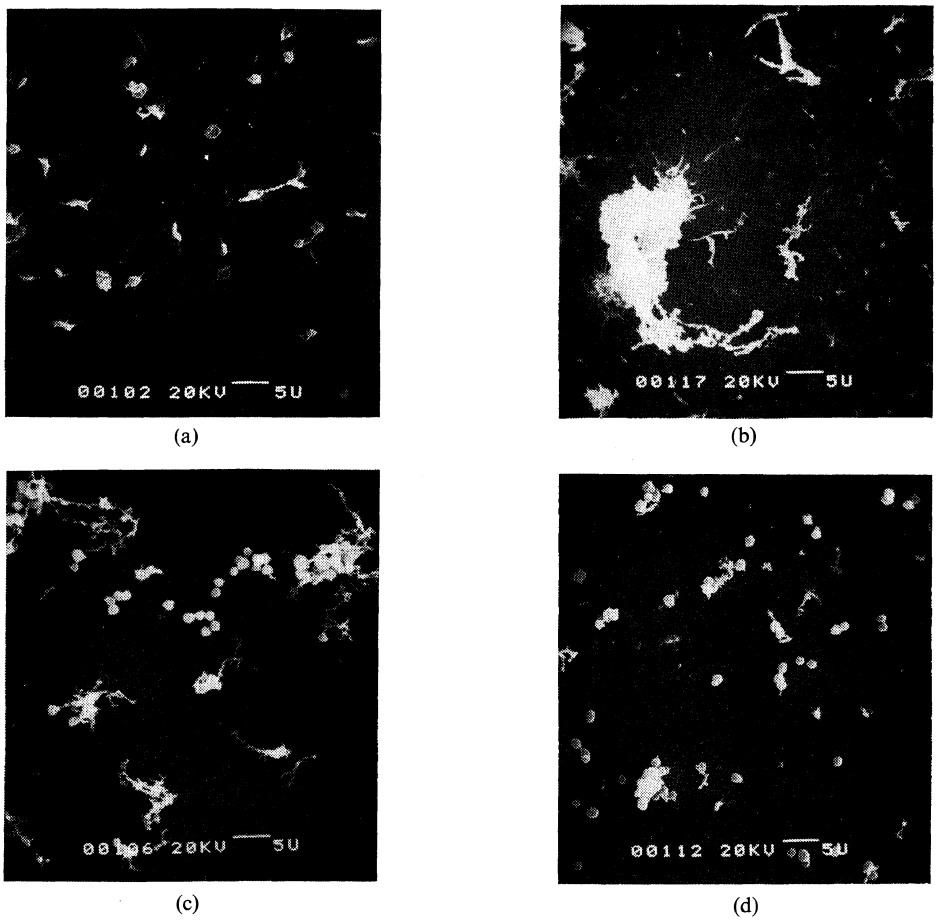

Figure 8. SEM micrographs of *in vitro* platelet deposition on (a) SBP-12/C, (b) SBP(Q)-12/C, (c) SB(X)P(Q)-12/C, and (d) S(S)B(X)P(Q)-12/C at 20 min contact. The few platelets on SBP-12/C are not activated while platelet deposition/aggregation is higher on the other materials.

Table III. Contact angle and ESCA results

Sample	Contact angle			ESCA			
	θ Water–air	θ Water–octane	γ_{sw} / dyn cm^{-2}	N/C	S/C	Br/C	Cl/C
SBP-10/C	27	34	1.5	0.025	—	—	—
SBP-10/B	39	48	3.4	0.016	—	—	—
SBP-12/C	33	30	1.6	0.020	—	—	—
SBP-12/B	33	43	2.4	0.010	—	—	—
SBP(Q)-12/C	18	Spread	—	0.0084	—	0.0089	—
SB(X)P(Q)-12/C	13	Spread	—	0.0033	0.010	0.0048	0.0074
S(S)B(X)P(Q)-12/C	15	Spread	—	0.0034	0.039	0.0053	0.0083

Table IV. ATR-IR absorbance ratios

Sample	$\frac{A_{1595}}{A_{1495}}$ (pyridine)	$\frac{A_{1640}}{A_{1495}}$ (quat. salt)	$\frac{A_{3400}}{A_{1495}}$ (N–H stretch)	$\frac{A_{911}}{A_{1495}}$ (1,2 vinyl)	$\frac{A_{963}}{A_{1495}}$ (1,4 *trans* C=C)	$\frac{A_{1200}}{A_{1495}}$ (O=S=O)
SBP-10/C	1.89	—	0.19	0.38	1.12	—
SBP-10/B	1.77	—	0.16	0.35	1.07	—
SBP-12/C	3.31	—	0.48	0.51	1.96	—
SBP-12/B	2.62	—	0.14	0.32	1.14	—
SBP(Q)-12/C	0.16	2.91	1.40	0.21	1.32	—
SB(X)P(Q)-12/C	0.07	0.82	0.20	—	—	—
S(S)B(X)P(Q)-12/C	0.08	0.80	0.20	—	—	0.56

more hydrophilic than polystyrene or polybutadiene, and thus a lower interfacial energy (γ_{sw}) is observed for SBP-10/C and SBP-12/C.

It was not possible to obtain interfacial energies for the modified polymers as octane bubbles spread on the surfaces of these materials. In addition, the water–air contact angles were low, indicating that the modified surfaces were more hydrophobic than the unmodified surfaces. The ESCA results indicate a significant decrease in surface nitrogen on the modified materials. It appears that the poly(4-vinylpyridine) phase may be partitioned in such a way that it is further from the surface than the other phases. Namely, the surface structure must have been altered by quaternization.

A result of crosslinking the butadiene phase is a reduction in surface bromine and an appearance of surface chlorine. This indicates that the counter ion of the quaternary ammonium salt was partly converted from Br^- to Cl^- in the process of crosslinking. The sulfur present on the surface of S(S)B(X)P(Q)-12/C is due to both the crosslinking agent used and the sulfonation reaction.

Table IV lists the various ATR-IR absorbance peaks of interest ratioed to the styrene absorbance peak at 1495 cm^{-1} (an internal standard), for the materials studied. An examination of the data for the unmodified polymers shows the SBP-12 materials to possess higher absorbances due to the pyridine ring (at 1595 and 3400 cm^{-1}). This is consistant with higher volume fractions of poly(4-vinylpyridine) (Table I). In addition, the polymers cast from chloroform (C) have higher pyridine ring IR absorbances than the same polymers cast from butyraldehyde and chloroform (B). This indicates that the surfaces of SBP-10/C and SBP-12/C are richer in the poly(4-vinylpyridine) phase than the corresponding SBP-10/B and SBP-12/B materials. These results are consistent with the contact angle and ESCA results in Table III.

Quaternization of SBP-12/C results in a reduced IR absorbance due to the pyridine ring (at 1595 cm^{-1}) but a new peak at 1640 cm^{-1} is due to the quaternary ammonium salt (Table IV). The dramatic reduction in the absorbance at 1595 cm^{-1} indicates almost complete quaternization. Interestingly, the N–H absorbance at 3400 cm^{-1} is very high for SBP(Q)-12, although the ESCA data in Table III shows a reduced surface level of nitrogen. This could be due to the vapor phase quaternization procedure used which can result in quaternization through the whole thickness of the coated polymer film. The penetration depth of the ATR-IR beam is much deeper (1000—10,000 Å) than the escape depth of electron in ESCA (50 Å), and thus ESCA is far more surface sensitive. The subsequent decrease of the 1595, 1640, and 3400 cm^{-1} bands on crosslinking and sulfonation (SB(X)P(Q)-12/C and S(S)B(X)P(Q)-12/C) indicate that

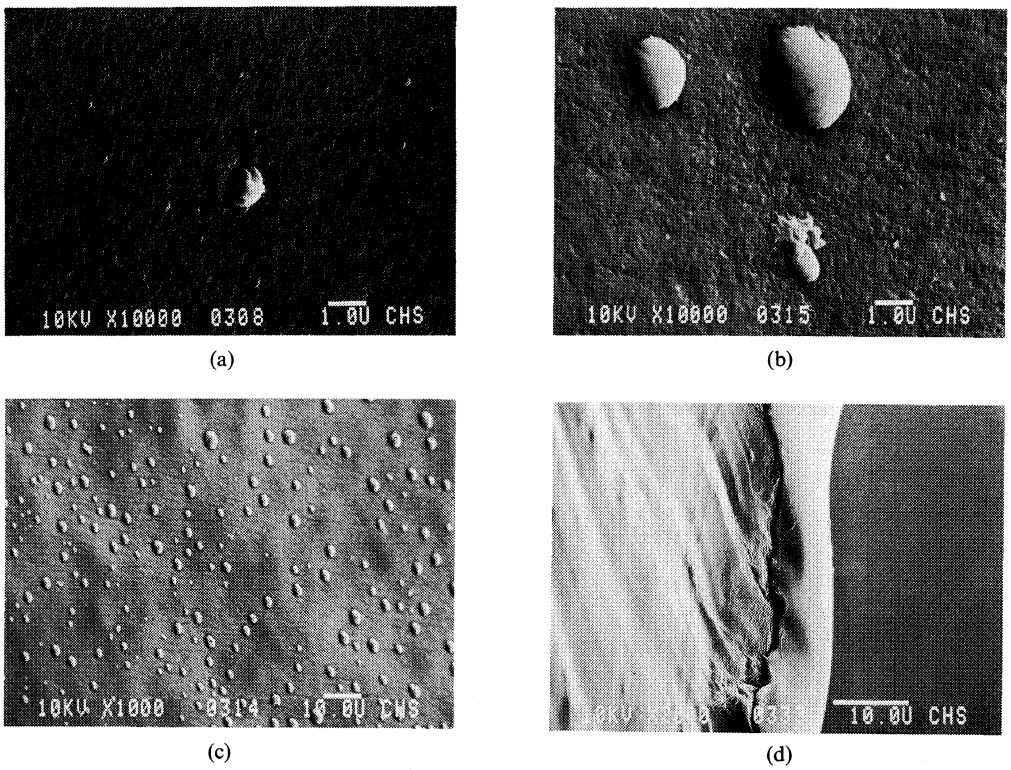

(a) (b) (c) (d)

Figure 9. SEM micrographs of (a) SBP-12/C surface showing microstructure, (b) and (c) S(S)B(X)P(Q)-12/C surface showing microstructure and protrusions, and (d) cross-sectional view of the polyethylene tubing showing coating of SBP-12/C.

quaternization may have been affected by these latter modifications. These decreases are consistent with the contact angle and ESCA results in Table III.

The ATR-IR results in Table IV also show that, as expected, crosslinking eliminated the absorption bands at 911 and 963 cm^{-1}. These bands are due to 1, 2 vinyl and 1,4 *trans* C=C groups, respectively. The broad band at about 1200 cm^{-1}, which corresponds to the O=S=O asymmetric stretch, appears on sulfonation (sample S(S)B(X)P(Q)-12/C).

SEM micrographs of the surfaces of SBP-12/C and S(S)B(X)P(Q)-12/C are shown in Figures 9a—c. The high resolution micrograph of the surface of SBP-12-C in Figure 9a is representative of all the materials, except S(S)B(X)P(Q)-12/C. In Figure 9a there appears to be microstructure on the order of 0.1 μm, with occasional larger 1 μm bumps. The high magnification of S(S)B(X)P(Q)-12/C (Figure 9b) also shows the microstructure on this surface. It is not clear whether the fine dots are actual pores, or regions of low electron density. However, superimposed on this microstructure are protrusions of 1—2 μm in diameter, regularly spaced on the surface of S(S)B(X)P(Q)-12/C, as shown in Figures 9b and c. These protrusions may be an artifact of the coating process, or due to block incompatibility, resulting in phase separation. It should be noted however, that phase separation determined on sectioned bulk polymer samples using transmission electron microscopy results in phases that are of the order of 400 Å in smallest dimension.[18]

In Figure 9d, a cross-section of the surface of SBP-12/C is shown. The coating is seen to

fold over the edge of the cut, onto the cross-sectional surface of the polyethylene tubing. This is due to deformation under the cutting stress. Nevertheless, this figure, and other views confirm the existence of an intact coating for this and for all the other materials studied. The thickness of the triblock polymer films are estimated to be 1—3 μm.

DISCUSSION

Blood Compatibility

The canine *ex vivo* series shunt experiment used in this study has been described in detail previously.[24] The technique is a useful model for the determination of the blood compatibility of a number of materials under conditions of flowing nonanticoagulated blood. The *ex vivo* technique allows for the simultaneous determination of the thromboembolitic potential of several materials under similar physiological and hematological conditions. This reduces the time and expense of animal testing, and requires fewer animals to obtain a substantial amount of *ex vivo* blood contact information. The effects of sample position in the series and cross-contamination have been addressed,[24] and found to be minimal under the experimental flow conditions.

The *ex vivo* results in Figures 2—5 show an increase in platelet and fibrinogen deposition to a peak at 15—20 min of blood contact, followed by a decrease to 10 min of blood contact. This general trend has been previously observed on a number of different surfaces.[6-8,24,26] The platelet peak height is used as a measure of blood compatibility — the higher the peak the poorer blood compatibility. Fibrinogen deposition generally follows the platelet deposition profiles. The *ex vivo* results in Figures 2—5 show that thrombogenicity is affected by both the casting solvent system, and by surface chemical modification. It should be noted, however, that the magnitudes of the platelet and fibrinogen peaks for the surfaces studied here are much greater than the polyethylene control (Table II) and much greater than those observed on a number of different polyurethanes.[6-8] The polymer systems studied here would thus be rather thrombogenic and are not likely to be found practically useful for blood-contacting applications. However, it is useful to study the effects of surface modification in order to further understand the mechanisms of blood-material interactions.

The *ex vivo* SEM results (Figures 6 and 7) complement the radiolabeling data (Figures 2—5). The sequence of platelet deposition and aggregation, thrombus formation, growth and embolization are observed in Figures 6 and 7. The thrombi formed on the surface of SBP(Q)-12/C at 15 min (Figure 7c) are composed of platelets, red cells, leukocytes and an occasional fibrin mesh. By 60 min of blood contact (Figure 7d) the surface is covered with spread leukocytes. This behavior has been observed on other very thrombogenic surfaces,[25,26,33-35] Leukocytes can migrate to the surface due to the release of chemotactic agents by the thrombi, and these cells may aid in the detachment of thrombi. Leukocyte spreading may be due to the activation of the leukocytes, but adhesive proteins such as fibronectin may also induce spreading.[25]

The *in vitro* results in Table II and Figure 8 are similar to the *ex vivo* results (Figures 2—7) in that the surface modified polymers demonstrate shorter clotting times, higher extents of contact activation, and high levels of platelet deposition and activation. A comparison of the *ex vivo* and *in vitro* results shows, however, that the *ex vivo* data is more sensitive to surface modification. Quaternization of SBP-12/C resulted in a 4.5-fold increase in peak platelet deposition, but only a 1.9-fold decrease in clotting time, and a 1.8-fold increase in contact activation time (Table II). It is also interesting to compare *in vitro* platelet deposition (Figure 8) with *ex vivo* platelet deposition (Figures 6 and 7). From the experiments conducted here it appears that the

in vitro results can predict gross relative trends, but the *in vitro* results are less sensitive measures of blood compatibility.

Effect of Solvent Casting

The polymers cast from chloroform (SBP-10/C and SBP-12/C) are more thromboresistant than those cast from a butyraldehyde and chloroform mixture (SBP-10/B and SBP-12/B) as shown in Figures 2 and 3, and Table II. From transmission electron microscope studies on thin sections of bulk material, the former polymers demonstrated ball-in-the-box morphologies, while the latter polymers possess trilayer lamellar morphologies.[17,19] It was not, possible, however, to distinguish surface morphology using SEM in the present study.

The contact angle, ESCA and ATR-IR data in Tables III and IV show that the polymers cast from chloroform are more hydrophilic and contain more surface nitrogen than those cast from the butyraldehyde/chloroform mixture. Hydrophilicity has been associated with blood compatibility[1,14] so it may be possible to explain trends in the data presented here on the basis of relative hydrophilicity. However, in absolute terms, the polymers studied are quite hydrophilic and yet are thrombogenic. The primary conclusion from this section is that choice of solvent affects both bulk and surface morphology and blood compatibility.

Effect of Chemical Modification

Quaternization of the pyridine blocks was found to drastically increase the thrombogenicity of SBP-12/C (Figures 4 and 5, and Table II). Subsequent crosslinking and sulfonation appeared to have little further effect on the blood response. Although negative surface charge has been long associated with blood compatibility,[36-38] there are some important exceptions.[28,39,40] The reason for the contradictions may be related to differences in chemical type and distributions of ionic groups or charge on the surface.[7,28,40] Previous work[7] has suggested that the presence of both positive and negative charges may lead to thromboresistant materials. In the previous study with polyurethanes,[7] positive and negative charges situated within the same hard segment phase improved blood compatibility. In the present study, the positive and negative charges are situated in different phases, giving rise to a charge mosaic configuration.[41] This did not improve blood compatibility. However, the polymers studied contained a high amount of poly(4-vinylpyridine) compared to the amount of poly(styrene) present. The pyridine blocks are more easily quaternized than the styrene blocks sulfonated, leading to a gross imbalance in the charge distribution. Further work should be directed toward examining samples with smaller levels of poly(4-vinylpyridine).

Acknowledgement. The authors acknowledge the assistance of Linda K. Lambrecht (animal surgery), Jeffrey A. Pierce (contact angles), Arlene P. Hart (hematology) and Carol A. Jordan (electron microscopy). The work was supported in part by a U.S.-Japan grant sponsored by the National Science Foundation through grant INT 801-16523 and the Japan Society for the Promotion of Science. Michael D. Lelah and Stuart L. Cooper also wish to acknowledge support of their biomaterials research by the National Institutes of Health through grant HL 21001. Tadao Kotaka wishes to acknowledge with thanks, support from the Ministry of Education, Science and Culture (Mombusho) through grants 5719009, 58211010, and 59105006 (the program coordinator, Prof. A. Nakajima, Kyoto University).

REFERENCES

1. J. D. Andrade, *Trans. Am. Soc. Artif. Intern. Organs*, **27**, 659 (1981).
2. A. S. Hoffman, *ACS Adv. Chem. Ser.*, **199**, 3 (1982).
3. D. J. Lyman, K. G. Klein, J. L. Brash, and B. K.

Fritzinger, *Thromb. et Diathes. Haemorrh.*, **22**, 120 (1970).
4. E. W. Merrill, V. sa da Costa, E. W. Salzman, D. Brier-Russell, L. Kuchner, D. F. Waugh, G. Trudel, S. Stopper, and V. Vitale, *ACS Adv. Chem. Ser.*, **199**, 95 (1982).
5. S. R. Hanson, L. A. Harker, B. D. Ratner, and A. S. Hoffman, *J. Lab. Clin. Med.*, **95**, 289 (1980).
6. M. D. Lelah, L. K. Lambrecht, B. R. Young, and S. L. Cooper, *J. Biomed. Mater. Res.*, **17**, 1 (1983).
7. M. D. Lelah, J. A. Pierce, L. K. Lambrecht, and S. L. Cooper, submitted to *J. Coll. Inter. Sci.* (1984).
8. M. D. Lelah, J. C. Conti, J. A. Pierce, L. K. Lambrecht, and S. L. Cooper, submitted to *Biomaterials* (1984).
9. A. Takahara, J. Tashita, T. Kajiyama, and M. Takayanagi, *Rep. Prog. Polym. Phys. Jpn.*, **24**, 737 (1981).
10. T. Okano, K. Kataoka, Y. Sakurai, M. Shimada, T. Akaike, and I. Shinohara, *Artificial Organs (Suppl.)*, **5**, 468 (1981).
11. M. Shimada, M. Miyahara, H. Tahara, I. Shinohara, T. Okano, K. Kataoka, and Y. Sakurai, *Polym. J.*, **15**, 649 (1983).
12. M. N. Helmus, O. P. Malhotra, and D. F. Gibbons, *ACS Adv. Chem. Ser.*, **199**, 81 (1982).
13. M. V. Sefton and E. W. Merrill, *J. Biomed. Mater. Res.*, **10**, 33 (1976).
14. T. Okano, S. Nishiyama, I. Shinohara, T. Akaike, Y. Sakurai, K. Kataoka, and T. Tsuruta, *Polym. Prepr.*, **20**, 571 (1979).
15. T. Fujimoto, *Design of Multiphase Biomedical Materials, Jpn.*, 48 (1983).
16. T. Kotaka and H. Ohnuma, *Design of Multiphase Biomedical Materials, Jpn.*, 54 (1983).
17. K. Arai, T. Kotaka, Y. Kitano, and K. Yoshimura, *Macromolecules*, **13**, 1670 (1980).
18. K. Arai, C. Ueda-Mashima, T. Kotaka, K. Yoshimura, and K. Maruyama, *Polymer*, **25**, 230 (1984).
19. I. Kudose and T. Kotaka, *Macromolecules*, **17**, 2325 (1984).
20. H. Ohnuma, I. Kudose, T. Shimohira, and T. Kotaka, *Rep. Prog. Polym. Phys. Jpn.*, **25**, 237 (1982).
21. I. Kudose, K. Arai, and T. Kotaka, *Polym. J.*, **16**, 241 (1984).
22. A. Ohnuma, H. Tanisugi, and T. Kotaka, *Rep. Progr. Polym. Phys. Jpn.*, **27**, 000 (1984).
23. T. Fujimoto, K. Ohkoshi, Y. Miyaki, and M. Nagasawa, *Science*, **224**, 74 (1984).
24. M. D. Lelah, L. K. Lambrecht, and S. L. Cooper, *J. Biomed. Mater. Res.*, **18**, 475 (1984).
25. M. D. Lelah, C. A. Jordan, M. E. Pariso, L. K. Lambricht, S. L. Cooper, and R. M. Albrecht, *SEM, IV*, 1983 (1983).
26. M. D. Lelah, C. A. Jordan, M. E. Pariso, L. K. Lambrecht, R. M. Albrecht, and S. L. Cooper, "Relationship to Surface Properties," *in* Polymers as Biomaterials, S. H. Shalaby and T. A. Horbett, Ed., ACS, 1984, in press.
27. M. M. Wintrobe, "Clinical Hamatology," Lea and Febiger, Philadelphia, 1956.
28. T. Matsuda, K. Uchida, H. Takano, K. Hayashi, Y. Taenaka, M. Umezu, T. Nakamura, and T. Akutsu, Proceedings of IUPAC Macromolecules, 1982, p 352.
29. G. E. Muilenberg, Ed., "Handbook of X-ray Photoelectron Spectroscopy," Perkin-Elmer Corp., Minnesota, 1979.
30. W. C. Hamilton, *J. Coll. Int. Sci.*, **10**, 219 (1972).
31. M. D. Lelah, J. A. Pierce, and S. L. Cooper, *J. Biomed. Mater. Res.*, **00**, 000 (1984).
32. J. D. Andrade, S. M. Ma, R. N. King, and D. E. Gregonis, *J. Coll. Int. Sci.*, **72**, 488 (1979).
33. R. D. Cumming, *Trans. Am. Soc. Artif. Intern. Organs*, **26**, 304 (1980).
34. B. H. Vale and R. T. Greer, *J. Biomed. Mater. Res.*, **16**, 471 (1982).
35. C. L. Van Kampen, D. F. Gibbons, and R. O. Jones, *J. Biomed. Mater. Res.*, **13**, 517 (1979).
36. P. N. Sawyer and J. W. Pate, *Am. J. Physiol.*, **175**, 118 (1953).
37. P. S. Chopra, S. Srinivasan, T. Lucas, and P. N. Sawyer, *Nature*, **215**, 1694 (1967).
38. J. E. Lovelock and J. S. Porterfield, *Nature*, **167**, 39 (1951).
39. M. C. Musolf, V. Metevia, and V. D. Hulce, *NIH PB*, **190**, 666 (1969).
40. H. L. Nossel, G. D. Wilner, and E. C. LeRoy, *Nature*, **221**, 75 (1969).
41. After this article has been submitted, T. K. was notified that Miyake *et al.* successfully tested the mosaic-charge effect of their pentablock copolymers for preventing platelet adhesion. However, their method involved only *in vitro* tests: H. Miyake, Y. Miyaki, K. Se, and T. Fujimoto, *Jpn. J. Artif. Organs*, **13**, 1243 (1984).